Available online at www.sciencedirect.com
SCIENCE DIRECT®
Tetrahedron: *Asymmetry* 16 (2005) 1061–1069
Tetrahedron: *Asymmetry*

β-Turn peptidomimetics incorporating $i + 1 - i + 3$ residues: solid phase syntheses and conformational properties

Samuel J. Reyes and Kevin Burgess*

Texas A&M University, Chemistry Department, PO Box 30012, College Station, TX 77842, USA

Received 21 December 2004; accepted 11 January 2005

Abstract—Solid phase syntheses of compounds **1** were developed. These gave the products in high crude purities, with little or no detectable head-to-tail dimer contaminants. NMR and CD data, interfaced with computational simulations, indicate these molecules sample β-turn conformations in solution.

1. Introduction

Cyclic peptidomimetic molecules containing constrained di- or tripeptide fragments can be useful for several applications.[1–6] In studies of protein–protein interactions[7,8] they are particularly valuable when both the amino acid sequence and the conformation at the contact points ('hot-spots') are known. For instance, nerve growth factor (NGF, Fig. 1) is an important target for medicinal chemistry. Interaction of this with its TrkA receptor involves the highlighted β-turn regions. Peptidomimetics that have the same amino acids and conformations as these turn regions therefore may bind to TrkA, and be used as pharmacological probes for this receptor, and/or as leads to therapeutics that mimic or disrupt the action of NGF.[9]

Structures **A**–**C** are peptidomimetics designed in our laboratories to mimic β-turns like those in NGF. Our strategy is to develop solid-phase syntheses of focused libraries of these compounds. Ideally, samples cleaved from the supports should be sufficiently pure for primary assays without purification (typically >85%). Solid-phase syntheses of systems **A**–**C** (which are 14-membered rings) have been reported.[10,11] These all gave 28-membered ring by-products wherein two strands had combined in a head-to-tail fashion. Alternative designs for which the desired ring closure is more facile, and formation of the undesired head-to-tail contaminants is suppressed, are potentially interesting.

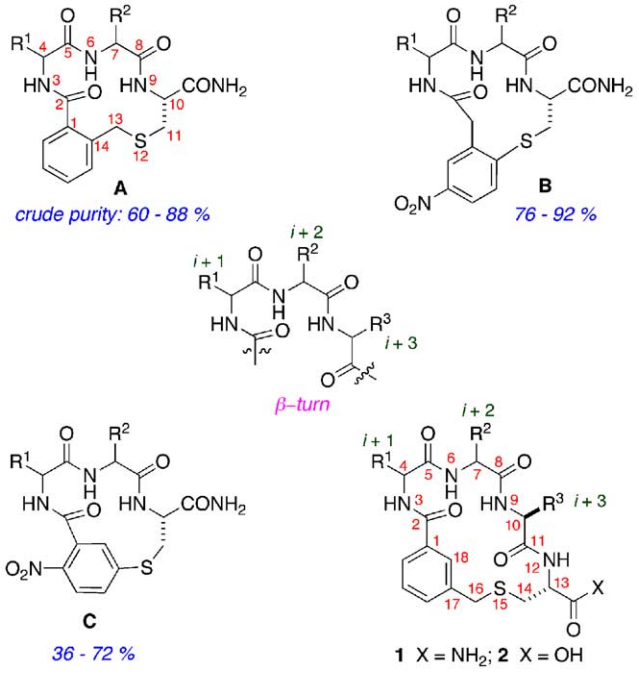

This paper features the turn mimics **1** and **2**. These structures are significantly different to **A**–**C** insofar as they incorporate one more amino acid residue. This could be a considerable advantage if the hot-spot involves the $i + 3$ residue of a β-turn. Consequently, the first objective of this work was to develop solid-phase syntheses that gave crude materials in high purities, preferably avoiding complications from head-to-tail

* Corresponding author. Tel.: +1 9798454345; fax: +1 9798458839; e-mail: burgess@tamu.edu

0957-4166/$ - see front matter © 2005 Elsevier Ltd. All rights reserved.
doi:10.1016/j.tetasy.2005.01.008

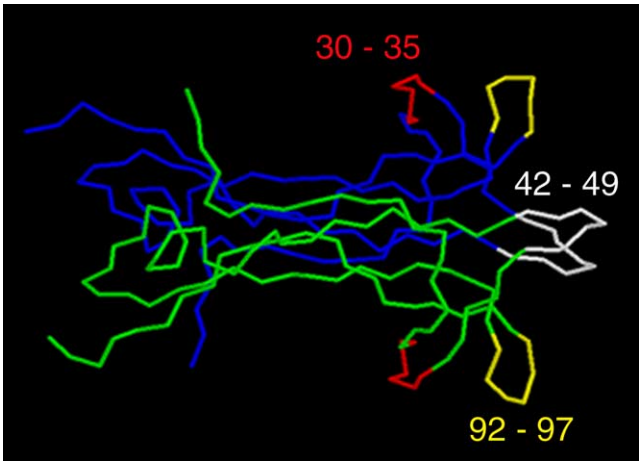

Figure 1. RASMOL diagram of the NGF dimer with the β-turn regions highlighted; the numbers show the amino acids highlighted.

macrocyclizations. At the onset of this study it was unclear that this could be done, especially since the ring size involved is larger (18 members). The second objective of this work was to test if these molecules populate β-turn conformations in solution.

2. Results and discussion

The methods used are shown in Scheme 1. Standard peptide synthesis methods were used to prepare the tetrapeptide precursors **D** via di-*iso*-propylcarbodiimide (DIC)/HOBt couplings of FMOC-protected amino acids[12,13] to polystyrene-based resins bearing the Wang or Rink handles (to obtain *C*-terminal carboxylates or amides, respectively).[14] The first amino acid added was cysteine with the side chain protected by monomethoxytrityl (Mmt) group.[15] The protected, supported tetrapeptides **D** were then acylated with 3-bromomethylbenzoyl chloride (made by forming the acyl chloride of 3-bromomethyl benzoic acid)[16] as shown. The Mmt group was removed from the intermediates **E** by acid treatment that was mild enough to exclude cleavage of other side-chain protection, and/or of the Wang or Rink handles. Treatment of the liberated thiol with $^{i}Pr_2NEt$ facilitated macrocyclization, and the products **1** and **2** were then cleaved from the resin by treating it with concentrated trifluoroacetic acid in CH_2Cl_2 in the presence of tri-*iso*-propylsilane (TIS) scavenger.

Nine different supports were screened for three peptidomimetic syntheses to assess the effect of the polymer used on the crude purities syntheses; the data is collected in Table 1. Interpretation of the results is complicated by the fact that different loadings were used. We considered adjusting the loadings to make them similar. However, this was not done because the purpose of this study was simply to find the most appropriate resin for our synthesis, used directly from the supplier without reducing the loading. Moreover, the loading levels for the SynPhase lanterns are hard to compare with the rest. In any event, the data for the free resins is quite similar,

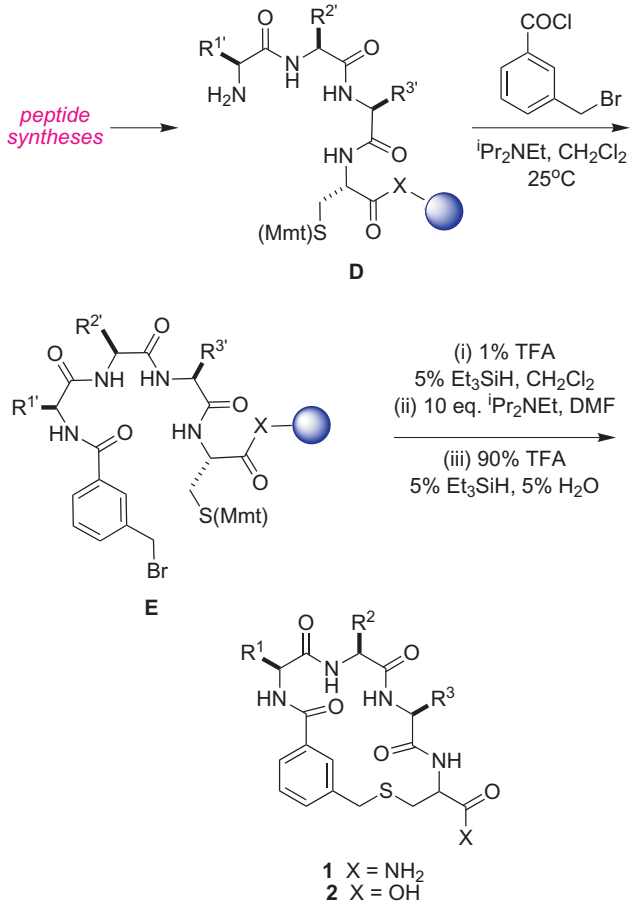

Scheme 1. Solid phase syntheses of **1** and **2**. $R^{1'}$, $R^{2'}$, and $R^{3'}$ are *protected* side chains where necessary. R^1, R^2, and R^3 are not protected.

the main difference in purities of the crude materials seems to correlate more with the handle used (Rink or Wang) than with the structure of the support itself. Purities of materials isolated from the SynPhase crowns were lower, but that could well be due to specific experimental modifications that are desirable for this particular support, that we perhaps did not find in our generalized approach.

Ultimately, TentaGel S RAM resin (which has a Rink handle) was selected and used to prepare the compounds shown in Table 2. The crude purities obtained show some sequence dependence on the sequence of amino acids encapsulated in the peptidomimetics. Generally, however, the purities of the products were satisfactory. HPLC and MS analyses indicate that macrocyclic head-to-tail combinations accounted for extremely minor or undetectable impurities, implying the cyclization to form products **1** is relatively efficient.

2.1. Conformational analyses of compounds 1a and 1g

All measurements were performed using DMSO-d_6 solvent for solubility reasons. In experiments to determine chemical shift coefficients, the GlyNH of **1a** gave a value of 3.3 ppb K^{-1}. This is just above the 3.0 ppb K^{-1};

Table 1. Crude purities for three peptidomimetics as a function of support and handle

Resin		Loading (mmol/g)	Supplier	AA^1–AA^2–AA^3		
				NKK % purity UV (Sedex)	ENN % purity UV (Sedex)	DGK % purity UV (Sedex)
Tenta Gel S RAM Fmoc	Rink	0.30	Advanced ChemTech	99 (96)	88 (94)	66 (75)
Tenta Gel S RAM Fmoc	Rink	0.22	Rapp Polymere	90 (93)	88 (93)	91 (97)
Argo Gel Rink NH Fmoc	Rink	0.33	Argonaut	95 (99)	88 (96)	83 (91)
Hypo Gel 400 RAM	Rink	0.53	Rapp Polymere	94 (99)	88 (95)	82 (88)
Rink Amide MBHA	Rink	0.61	NovaBiochem	95 (98)	89 (94)	85 (94)
Synphase Lantern	Rink	0.036	Mimotopes	75(91)	67 (84)	89 (92)
Tenta Gel S AC	Wang	0.24	Rapp Polymere	90 (84)	83 (97)	44 (52)
Hypo Gel 400 PHB	Wang	0.61	Rapp Polymere	82 (95)	67 (76)	56 (67)
Nova Syn TGA	Wang	0.25	NovaBiochem	90 (100)	36 (29)	—[a]

[a] Analysis complicated by an impurity.

Table 2. Crude purities and isolated yields for the peptidomimetics

Compound	Sequence	Purity (%)		Isolated yield (%)
		UV	Sedex	
1a	IKG	92	95	27
1b	DIK	72	77	45
1c	NNS	92	97	16
1d	INN	93	92	29
1e	DGK	66	75	69
1f	GKQ	81	84	16
1g	IRG	87	91	36
1h	DIR	83	79	34
1i	KTG	91	89	68
1j	NNK	97	97	21
1k	ENN	89	94	46
1l	NKQ	64	67	36
1m	DNK	67	81	20

measurements below this value are usually considered to be indicative of solvent shielding and/or H-bonding, so the 3.3 ppb K^{-1} is inconclusive.[17,18] Quenched molecular dynamics (QMD) calculations[19,20] were performed to provide a physical model to compare with the spectroscopic data obtained for **1a**. We have applied this technique to similar systems before, and described the procedure in detail.[21–23] Briefly, this technique generates a virtual set of conformational families, reminiscent of equilibrating conformers of the molecule. Significantly, no spectral measurements are used to generate this model, so good agreement with experimentally observed parameters is indicative of a realistic model. The results of the QMD and NMR studies for **1a** are shown in Table 3.

QMD simulations for **1a** in DMSO afforded three families of conformers. Family 1 (by definition) contains the overall lowest energy conformer that was generated, and it was also the most populated. The lowest energy conformer Φ, Ψ angles for the $i+1$ residues (Ile), and the Φ angle for the $i+2$ (Lys) residue (−74°, −37°, and −95°, respectively) compare well with those for an ideal type I β-turn (−60°, −30°, −90°).[24] The Ψ value for the $i+2$ deviates from the ideal (-22_{calcd} vs 0_{ideal}°), but our

Table 3. Data from conformational analysis of peptidomimetic **1a**

Residue		Dihedral angles for lowest energy conformers (degrees)		
		Family 1	Family 2	Family 3
QMD data				
Ile	Φ	−74.32	−73.27	−165.8
	Ψ	−36.92	−25.85	−43.68
Lys	Φ	−95.28	−95.32	−143.0
	Ψ	−22.36	−42.93	−13.77
Number in family		69	29	5
Lowest energy conformer (kcal mol^{-1})		−8.358	−6.946	−5.7236
CO_i–NH_{i+3} distance (Å)		3.096	3.376	5.354

Contacts/characteristic	ROE intensity	Calcd. dist. from QMD (Å)
Fit of lowest energy conformer from family 1 with NMR data		
(Aryl)*H*–(Ile)N*H*	Strong	1.844
(Ile)N*H*–(Lys)N*H*	Medium	2.283
(Lys)N*H*–(Gly)N*H*	Weak	2.079
(Gly)N*H*–(Cys)$C_\alpha H$	Not obsd.	3.030
(Ile)$C_\alpha H$–(Lys)N*H*	Not obsd.	3.486
(Lys)$C_\alpha H$–(Gly)N*H*	Not obsd.	3.458
	$^3J_{obsd}$ (Hz)	$^3J_{calcd}$ (Hz)
(Ile)$C_\alpha H$–N*H*	7.9	6.0
(Lys)$C_\alpha H$–N*H*	8.3	8.4

prior research in this area has shown that this is common for constrained peptidomimetics of this kind.[23] That lowest energy conformer has a CO_i–NH_{i+3} distance (Å) of about 3 Å, and this is also indicative of a β-turn.

Having established that the simulations indicate **1a** has a preference for a type I β-turn conformation, the next step is to compare the data for the simulated low-energy conformer with experimentally determined parameters. Comparison of ROE[25] crosspeaks with the simulated distances for this low-energy conformer (Table 3) reveals an acceptable correspondence. None of the low-energy conformers from the other families fit the ROE data as well as this (data not shown). Further, comparison of the observed coupling constants for the $i + 1$ and $i + 2$ residues reveals a reasonably good fit. Figure 2a shows the lowest-energy conformer obtained from the QMD studies of **1a**.

Circular dichroism (CD) spectra were also obtained to acquire more information about the conformational preferences of peptidomimetics **1a** and **1g**. Informative CD data cannot be obtained using DMSO as solvent, so a 4:1 water/methanol mixture with the same dielectric was used. Figure 2b shows the spectra obtained. Both peptidomimetics give a low wavelength minimum and a higher wavelength maximum characteristic of type I β-turns, though the peaks are red shifted by around 20 nm relative to the ideal.[26] CD data alone do not provide definitive proof of a β-turn conformation, but we feel the data obtained here support a populated type I turn conformation for **1a**. Contributions from the constrained aromatic ring in this structure may be a factor to the red shift that is observed relative to β-turns based exclusively on peptides.

The CD data for **1a** and **1g** are similar, implying the latter compound may also populate similar turn conformations. We believe this assertion is supported by data from QMD/NMR studies (Table 4), though it is somewhat harder to interpret. QMD studies of **1g** gave two major families of conformers. The lowest energy conformers of those two families are quite similar (Fig. 2c), and in both cases the Φ, Ψ angles for the $i + 1$ residues (Ile), and the Φ angle for the $i + 2$ (Arg) residue (−74°, −37°, and −95°, respectively) are reasonably close to an ideal type I β-turn (−60°, −30°, −90°). For both conformers, the CO_i–NH_{i+3} distances measured imply close contact as observed in β-turns.

Temperature coefficient studies for the Gly N*H* proton of **1g** gave a value of 2.8 ppb K^{-1} indicative of H-bonding or solvent shielding. The ROE data for **1g** correlates well with the distances observed for the low-energy conformer from family 2, but there is a deviation for the (Aryl) *H*–(Ile) N*H* for the lowest energy overall (i.e., from family 1). The observed and simulated coupling constants for the $i + 1$ and $i + 2$ $C_\alpha H$–N*H* parameters are closest for family 1, and the worst deviation for family 2 is less than 2.5 Hz. Overall, we conclude that peptidomimetic **1g** also populates type I β-turn conformations.

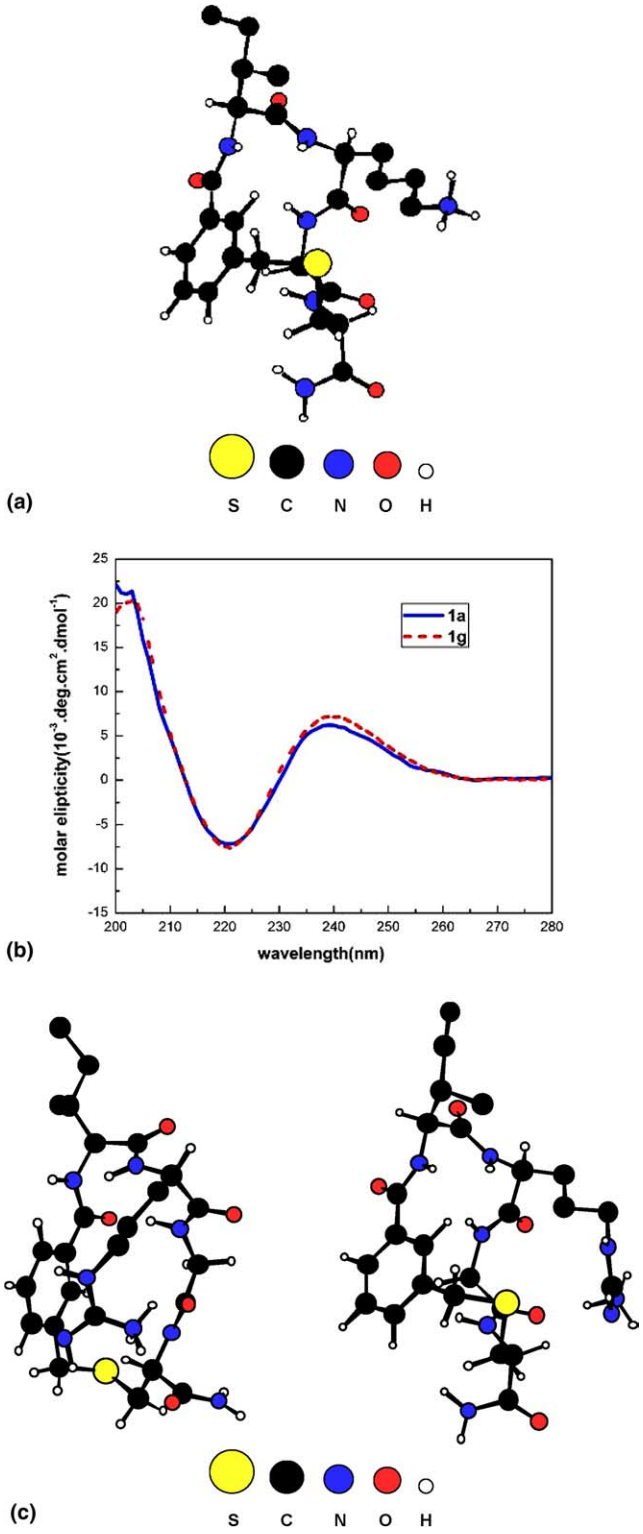

Figure 2. (a) Lowest energy conformer simulated for **1a**. (b) CD spectra of compounds **1a** and **1g** in 4:1 water/methanol at approximately 0.2 mg/mL. (c) Family 1 and 2 lowest energy conformers simulated for **1g**.

3. Conclusions

This work describes methods to obtain compounds **1** with relatively high crude purities. The head-to-tail

Table 4. Data from conformational analysis of peptidomimetic **1g**

Residue			Dihedral angles for lowest energy conformers (degrees)	
			Family 1	Family 2
QMD data				
Ile		Φ	−73.40	−73.57
		Ψ	−37.13	−29.89
Arg		Φ	−98.3	−72.13
		Ψ	−21.58	−15.93
Number in family			49	44
Lowest energy conformer (kcal mol^{-1})			9.926	10.39
CO_i–NH_{i+3} distance (Å)			3.117	2.344
Contacts/characteristic	ROE intensity		Calcd. dist. from QMD (Å)	
			Family 1	Family 2
Fit of lowest energy conformers, family 1 and 2, with NMR data				
(Aryl)*H*–(Ile)N*H*	Strong		4.471	1.827
(Ile)N*H*–(Arg)N*H*	Medium		2.310	2.234
(Arg)N*H*–(Gly)N*H*	Weak		2.042	2.520
(Gly)N*H*–(Cys)C$_\alpha$*H*	Not obsd.		3.204	3.858
(Ile)C$_\alpha$*H*–(Arg)N*H*	Not obsd.		3.490	3.459
(Arg)C$_\alpha$*H*–(Gly)N*H*	Not obsd.		3.453	3.418
	$^3J_{obsd}$ (Hz)		$^3J_{calcd}$ (Hz)	
(Ile)C$_\alpha$*H*–N*H*	7.9		5.9	5.9
(Arg)C$_\alpha$*H*–N*H*	8.1		8.7	5.7

'dimeric' macrocycles that were observed for systems like **A**–**C** were insignificant in these syntheses, even though the ring size is greater for systems **1**. Probably, enhanced conformational flexibility in the acyclic precursors for the systems presented here better enable them to adopt the conformations necessary for ring closure. Conformational studies for compounds **1a** and **1g** indicate they can adopt states that closely resemble natural type I β-turn motifs.

4. Experimental

4.1. General methods

All α-amino acids used have the L-configuration and were purchased from NovaBiochem, Advanced ChemTech or Chem-Impex. Chemicals were obtained from commercial suppliers and used without further purification. Di-*iso*-propylcarbodiimide (DIC), *N*-hydroxybenzotriazole (HOBt), trifluoroacetic acid (TFA), oxalyl chloride, diisopropylethylamine (DIEA), piperidine, and triisopropylsilane (TIS) were purchased from Aldrich. Dimethylformamide (DMF), methanol, and dichloromethane were bought from EMScience. The resins were obtained from Rapp Polymere, Advanced ChemTech, Nova Biochem, Argonaut Technologies, and Chiron Mimetopes.

Peptidomimetic syntheses were performed in fritted polypropylene syringes (5 mL capacity) from Torviq. Reverse-phase high-performance liquid chromatography (HPLC) analyses were carried out using a Beckman SystemGold instrument and a Vydac C-18 column (catalog no. 218TP54, length: 250 mm; inner diameter: 4.6 mm). Preparative purifications were done on an SSI HPLC system using a Vydac C-18 column (catalog no. 2181022, length: 250 mm, inner diameter: 22 mm). All HPLC analyses were done under gradient conditions. Eluents used were solvent A (H_2O with 0.1% TFA) and solvent B (CH_3CN with 0.1% TFA). Flow rates applied were 1.0 and 6 mL/min for analytical and preparative HPLC, respectively.

4.2. Typical solid-phase syntheses of peptidomimetics: the IKG derivative 1a

In a 5 mL fritted syringe, TentaGel S RAM Fmoc (0.05 mmol, 0.30 mmol g^{-1}) was swelled in DMF (ca. 10 mL g^{-1}) for 1 h. The resin was washed with DMF (3× ca. 10 mL g^{-1}, each time for 1 min; this amount of solvent and washing time were used for all other washings throughout). The Fmoc protecting group was removed by treating the resin with 20% piperidine in DMF (2×, first 10 min, then for 20 min). The resin was washed with DMF (3×), MeOH (3×) and CH_2Cl_2 (3×), after which a solution of FmocCys(Mmt)–OH (3 equiv), DIC (5 equiv) and HOBt (5 equiv) in 1.5 mL DMF was added. After shaking for 10 h, a Kaiser test[27] on sample beads indicated a negative result. The reaction mixture was drained and the resin washed with DMF (3×). The above deprotection, coupling, and washing cycles were repeated to attach FmocGly–OH, FmocLys–OH, and FmocIle–OH. After the final Fmoc deprotection, the resin was washed with DMF (3×), MeOH (3×), and CH_2Cl_2 (3×). The resin was dried for 2 h in vacuo, then a solution of 3-bromomethylbenzoylchloride (3 equiv) and DIEA (5 equiv) in 2 mL CH_2Cl_2 were added. After 1 h of shaking, a Kaiser test gave a negative result. The resin was washed with CH_2Cl_2 (5×). The Mmt group on cysteine was removed by treating the resin with 1% TFA and 5% TIS in CH_2Cl_2 (6×, each time for 10 min). The

resin was then washed with CH_2Cl_2 (4×) and DMF (3×). Cyclization was carried out by adding 10 equiv of DIEA in ca. 2.0–2.5 mL DMF and shaking the resin for 12 h. The resin was then washed with DMF (3×), MeOH (3×), and CH_2Cl_2 (3×) before it was dried for 2 h in vacuo. The product was cleaved by treating the resin with 90% TFA, 5% TIS, and 5% H_2O (ca. 3.5–4 mL) for 2–4 h. The resin was then washed with 50% TFA in CH_2Cl_2 (2×). The collected filtrate and washings were concentrated and the product was precipitated by adding Et_2O (ca. 3 mL). The white precipitate was isolated by centrifugation of the mixture and carefully decanting the ether. The crude peptide was then dissolved in the minimum volume of H_2O with a little CH_3CN added (total volume <2.5 mL) and was purified via preparative HPLC (SSI System, 20–30% B in 25 min). The dominant fraction was concentrated and lyophilized to give a white fluffy solid (7.2 mg, 27%). ^{1}H NMR (500 MHz, DMSO-d_6, 25 °C): δ = 8.41 (d, 7.94 Hz, 1H), 8.23 (d, 8.23 Hz, 1H), 8.07 (d, 8.30 Hz, 1H), 7.77 (s, 1H), 7.72–7.67 (m, 4H), 7.52–7.49 (m, 2H), 7.42 (t, 7.65 Hz, 1H), 7.24 (s, 1H), 4.41 (q, 7.46 Hz, 1H), 4.22–4.15 (m, 2H), 4.03 (dd, 7.22, 16.85 Hz, 1H), 3.90–3.82 (m, 2H), 3.59 (dd, 3.94, 16.85 Hz, 1H), 2.82–2.73 (m, 3H), 2.42 (dd, 7.44, 13.84 Hz, 1H), 1.96–1.90 (m, 1H), 1.88–1.83 (m, 1H), 1.67–1.60 (m, 1H), 1.58–1.51 (m, 3H), 1.37–1.26 (m, 2 H), 1.25–1.16 (m, 1H), 0.92 (d, 6.80 Hz, 3H), 0.88 (t, 7.59 Hz, 3H); ^{13}C NMR (75 MHz, DMSO-d_6, 25 °C): δ = 173.6, 171.6, 171.4, 171.1, 168.4, 168.0, 167.0, 158.3, 157.8, 139.2, 139.1, 135.4, 122.1, 117.2, 59.8, 52.8, 51.9, 42.5, 35.8, 30.6, 26.6, 25.2, 22.4, 15.6, 10.7; analytical HPLC: homogeneous single peak, t_R = 13.05 min (8–70% B in 30 min); MALDI MS: calcd for $C_{25}H_{38}N_6O_5S$ $\{M+H\}^+$ 535.67, found $\{M+H\}^+$ 535.20.

4.3. DIK derivative 1b

TentaGel S RAM Fmoc resin (0.05 mmol, 0.30 mmol g^{-1}) was used to synthesize this compound. After cleavage from the resin, the crude peptide was purified by preparative HPLC and was lyophilized to give a white fluffy solid (13.2 mg, 45%). ^{1}H NMR (300 MHz, DMSO-d_6, 25 °C): δ = 8.34 (d, 7.71 Hz, 1H), 8.25 (d, 7.71 Hz, 1H), 8.03 (d, 6.73 Hz, 1H), 7.80–7.74 (m, 2H), 7.70–7.63 (m, 2H), 7.55–7.41 (m, 3H), 7.29 (s, 1H), 7.26 (s, 1H), 4.98–4.90 (m, 1H), 4.81 (dd, 7.09, 15.05 Hz, 1H), 4.56–4.37 (m, 3H), 4.29–4.21 (m, 1H), 3.91–3.75 (m, 4H), 3.64–3.59 (m, 1H), 2.80–2.69 (m, 3H), 2.68–2.59 (m, 1H), 2.30 (dd, 6.04, 13.10 Hz, 1H), 1.63–1.46 (m, 2H), 1.41–1.23 (m, 2H), 1.17–1.03 (m, 1H), 0.85 (d, 6.88 Hz, 3H), 0.35 (d, 7.13 Hz, 3H); analytical HPLC: homogeneous single peak, t_R = 10.48 min (8–70% B in 30 min); MALDI MS: calcd for $C_{27}H_{40}N_6O_5S$ $\{M+H\}^+$ 593.71, found M+H$^+$ 593.19.

4.4. NNS derivative 1c

TentaGel S RAM Fmoc resin (0.05 mmol, 0.30 mmol g^{-1}) was used to synthesize this compound. After cleavage from the resin, the crude peptide was purified by preparative HPLC and was lyophilized to give a white solid (4.3 mg, 16%). ^{1}H NMR (500 MHz, DMSO-d_6, 25 °C): δ = 8.71 (d, 7.83 Hz, 1H), 8.28 (d, 7.26 Hz, 1H), 8.19 (d, 8.37 Hz, 1H), 7.85–7.83 (m, 2H), 7.72–7.70 (m, 1H), 7.49–7.51 (m, 1H), 7.46–7.43 (m, 3H), 7.41 (s, 1H), 7.24 (s, 1H), 6.93 (s, 2H), 4.85 (t, 5.86 Hz, 1H), 4.66–4.62 (m, 1H), 4.42 (q, 7.25 Hz, 1H), 4.32–4.28 (m, 1H), 4.26–4.22 (m, 1H), 3.89–3.79 (m, 2H), 3.72–3.68 (m,1H), 3.64–3.59 (m, 1H), 2.79–2.74 (m, 2H), 2.72–2.69 (m, 2H), 2.65–2.58 (m, 1H) 2.31 (dd, 2.31, 13.80 Hz, 1H); analytical HPLC: homogeneous single peak, t_R = 7.46 min (8–70% B in 30 min); MALDI MS: calcd for $C_{22}H_{29}N_7O_8S$ $\{M+Na\}^+$ 574.57, found $\{M+Na\}^+$ 574.11.

4.5. INN derivative 1d

TentaGel S RAM Fmoc resin (0.05 mmol, 0.30 mmol g^{-1}) was used to synthesize this compound. After cleavage from the resin, the crude peptide was purified by preparative HPLC and was lyophilized to give a white solid (8.3 mg, 29%). ^{1}H NMR (500 MHz, DMSO-d_6, 25 °C): δ = 8.45 (d, 9.15 Hz, 1H), 8.41 (d, 8.42 Hz, 1H), 8.22 (d, 8.65 Hz, 1H), 8.12 (d, 6.56 Hz, 1H), 7.73 (s, 1H), 7.67–7.65 (m, 1H), 7.54 (s, 1H), 7.52–7.48 (m, 3H), 7.42 (t, 7.55 Hz 1H), 7.23 (s, 1H), 7.03 (s, 1H), 6.97 (s, 1H), 4.50–4.46 (m, 1H), 4.41–4.34 (m, 2H), 4.23 (t, 9.75 Hz, 1H), 3.89–3.78 (m, 2H), 3.44–3.41 (m, 1H), 3.0 (dd, 6.70, 13.86 Hz, 1H), 2.69–2.63 (m, 1H), 2.61–2.54 (m, 2H), 2.39 (dd, 8.51, 13.86 Hz, 1H), 1.86–180 (m, 1H), 1.54–1.47 (m, 1H), 1.16–1.07 (m, 1H), 0.87 (d, 5.53 Hz, 3H), 0.85 (t, 7.24 Hz, 3H); analytical HPLC: homogeneous single peak, t_R = 12.61 min (8–70% B in 30 min); MALDI MS: calcd for $C_{25}H_{35}N_7O_7S$ $\{M+Na\}^+$600.65, found $\{M+Na\}^+$ 600.30.

4.6. DGK derivative 1e

TentaGel S RAM Fmoc resin (0.05 mmol, 0.30 mmol g^{-1}) was used to synthesize this compound. After cleavage from the resin, the crude peptide was purified by preparative HPLC and was lyophilized to give a white solid (18.6 mg, 69%). ^{1}H NMR (500 MHz, DMSO-d_6, 25 °C): δ = 12.3 (br s, 1H), 9.30 (d, 7.64 Hz, 1H), 8.25 (dd, 3.86, 8.56 Hz, 1H), 8.01 (s, 1H), 7.91 (d, 9.10 Hz, 1H), 7.80–7.78 (m, 1H), 7.71 (br s, 2H), 7.59 (d, 7.79 Hz, 1H), 7.50–7.45 (m, 2H), 7.29 (s, 1H), 7.24 (s, 1H), 4.55 (q, 6.79 Hz, 1H), 4.49–4.44 (m, 1H), 4.23–4.15 (m, 2H), 3.90–3.82 (m, 2H), 3.75–3.73 (m, 1H), 3.54–3.50 (m, 2H), 3.08 (dd, 6.68, 16.21 Hz, 1H), 2.83 (dd, 5.28, 12.24 Hz, 1H), 2.68 (dd, 6.68, 16.21 Hz, 1H), 2.18 (dd, 8.75, 12.24 Hz, 1H), 1.93–1.84 (m, 1H), 1.83–1.77 (m, 1H), 1.60–1.56 (m, 2H), 1.46–1.38 (m, 1H), 1.37–1.34 (m, 1H); analytical HPLC: homogeneous single peak, t_R = 9.26 min (8–70% B in 30 min); MALDI MS: calcd for $C_{23}H_{32}N_6O_7S$ $\{M+H\}^+$ 537.60, found $\{M+H\}^+$ 537.15.

4.7. GKQ derivative 1f

TentaGel S RAM Fmoc resin (0.05 mmol, 0.30 mmol g^{-1}) was used to synthesize this compound. After cleavage from the resin, the crude peptide was

purified by preparative HPLC and was lyophilized to give a white solid (18.6 mg, 69%). ^{1}H NMR (500 MHz, DMSO-d_6, 25 °C): δ = 8.64–8.63 (m, 2H), 8.52 (d, 8.68 Hz, 1H), 8.20 (d, 7.32 Hz, 1H), 7.90 (s, 1H), 7.76–7.70 (m, 4H), 7.50 (d, 7.26 Hz, 1H), 7.45 (t, 7.71 Hz, 1H), 7.29 (s, 1H), 7.26 (s, 1H), 6.77 (s, 1H), 4.67–4.62 (m, 1H), 4.28–4.24 (m, 2H), 4.04 (dd, 4.92, 14.50 Hz, 1H), 4.0–3.95 (m, 2H), 3.78–3.73 (m, 2H), 3.44–3.40 (m, 1H), 2.56 (dd, 9.89, 13.67 Hz, 1H), 2.18 (dd, 4.85, 13.67 Hz, 1H), 2.03 (t, 8.34 Hz, 2H), 1.90–1.85 (m, 1H), 1.81–1.74 (m, 2H), 1.72–1.63 (m, 1H), 1.60–1.48 (m, 2H), 1.44–1.29 (m, 2H); analytical HPLC: homogeneous single peak, t_R = 8.62 min (8–70% B in 30 min); MALDI MS: calcd for $C_{24}H_{35}N_7O_6S$ $\{M+Na\}^+$ 572.64, found $\{M+Na\}^+$ 572.15.

4.8. IRG derivative 1g

TentaGel S RAM Fmoc resin (0.05 mmol, 0.30 mmol g^{-1}) was used to synthesize this compound. After cleavage from the resin, the crude peptide was purified by preparative HPLC and was lyophilized to give a white solid (18.6 mg, 69%). ^{1}H NMR (500 MHz, DMSO-d_6, 25 °C): δ = 8.44 (d, 7.90 Hz, 1H), 8.22 (d, 8.36 Hz, 1H), 8.10 (d, 8.10 Hz, 1H), 7.77 (s, 1H), 7.73–7.70 (m, 2H), 7.57 (t, 5.7 Hz, 1H), 7.52–7.51 (m, 2H), 7.49 (s, 1H), 7.24 (s, 1H), 4.40 (q, 7.15 Hz, 1H), 4.22–4.15 (m, 2H), 4.04 (dd, 6.89, 16.70 Hz, 1H), 3.86 (q, 13.12 Hz, 2H), 3.59 (dd, 3.95, 16.70 Hz, 1H), 3.12 (q, 6.59 Hz, 2H), 2.79 (dd, 7.16, 14.05 Hz, 1H), 2.41 (dd, 7.16, 14.05 Hz, 1H), 1.96–1.85 (m, 2H), 1.68–1.61 (m, 1H), 1.53–1.49 (m, 2H), 1.47–1.40 (m, 1H), 1.25–1.15 (m, 1H), 0.92 (d, 6.81 Hz, 3H), 0.88 (t, 7.43 Hz, 3H); ^{13}C NMR (75 MHz, DMSO-d_6, 25 °C): δ = 174.1, 172.1, 171.8, 171.6, 168.9, 168.5, 167.5, 157.2, 139.7, 139.6, 135.8, 123.6, 122.6, 117.7, 60.3, 53.8, 52.4, 43.0, 36.2, 34.9, 32.9, 28.9, 25.7, 16.1, 11.1; analytical HPLC: homogeneous single peak, t_R = 13.45 min (8–70% B in 30 min); MALDI MS: calcd for $C_{25}H_{38}N_8O_5S$ $\{M+H\}^+$ 563.69, found $\{M+H\}^+$ 563.19.

4.9. DIR derivative 1h

TentaGel S RAM Fmoc resin (0.05 mmol, 0.30 mmol g^{-1}) was used to synthesize this compound. After cleavage from the resin, the crude peptide was purified by preparative HPLC and was lyophilized to give a white solid (18.6 mg, 69%). ^{1}H NMR (500 MHz, DMSO-d_6, 25 °C): δ = 10.84 (br s, 1H), 8.34 (d, 6.71 Hz, 1H), 7.78 (s, 1H), 7.66 (d, 7.18, 1H), 7.63 (d, 8.50 Hz, 1H), 7.47–7.45 (m, 3H), 7.37 (t, 6.95 Hz, 1H), 7.32–7.25 (m, 2H), 7.19–7.07 (m, 3H), 6.55 (s, 1H), 4.83–4.77 (m, 1H), 4.73–4.66 (m, 1H), 4.47–4.45 (m, 1H), 4.44 (dd, 6.54, 17.11 Hz, 1H), 3.76–3.71 (m, 3H), 3.42 (dd, 5.83, 11.10 Hz, 1H), 3.14–3.05 (m, 2H), 2.86–2.78, (m, 1H), 2.74–2.68 (m, 1H), 1.77–1.66 (m, 2H), 1.64–1.56 (m, 1H), 1.55–1.49 (m, 2H), 1.48–1.42 (m, 1H), 1.24–1.20 (m, 1H), 0.89 (d, 6.67 Hz, 3H), 0.86 (t, 7.17, 3H); analytical HPLC: homogeneous single peak, t_R = 10.87 min (8–70% B in 30 min); MALDI MS: calcd for $C_{28}H_{40}N_8O_7S$ $\{M+H\}^+$ 621.72, found $\{M+H\}^+$ 621.25.

4.10. KTG derivative 1i

TentaGel S RAM Fmoc resin (0.05 mmol, 0.30 mmol g^{-1}) was used to synthesize this compound. After cleavage from the resin, the crude peptide was purified by preparative HPLC and was lyophilized to give a white solid (17.7 mg, 68%). ^{1}H NMR (500 MHz, DMSO-d_6, 25 °C): δ = 8.45 (d, 7.94 Hz, 1H), 8.38 (d, 8.51 Hz, 1H), 8.17 (d, 7.76 Hz, 1H), 7.85 (d, 8.92 Hz, 1H), 7.78–7.70 (m, 3H), 7.57 (s, 1H), 7.51 (s, 1H), 7.44 (t, 7.78 Hz, 1H), 7.43–7.40 (m, 1H), 7.26 (s, 1H), 4.50–4.41 (m, 1H), 4.40–4.36 (m, 1H), 4.27–4.20 (m, 1H), 4.18 (dd, 2.47, 8.92 Hz, 1H), 4.04 (dd, 6.29, 16.92 Hz, 1H), 3.96–3.92 (m, 1H), 3.94–3.83 (m, 2H), 3.65 (dd, 3.71, 16.92 Hz, 1H), 2.90 (dd, 5.74, 14.03 Hz, 1H), 2.79 (unresolved, 1H), 2.42 (dd, 8.07, 14.03 Hz, 1H), 1.84–1.80 (m, 2H), 1.63–1.57 (m, 2H), 1.50–1.35 (m, 3H), 1.04 (d, 6.43 Hz, 3H); analytical HPLC: homogeneous single peak, t_R = 7.51 min (8–70% B in 30 min); MALDI MS: calcd for $C_{23}H_{34}N_6O_6S$ $\{M+H\}^+$ 523.62, found $\{M+H\}^+$ 523.34.

4.11. NNK derivative 1j

TentaGel S RAM Fmoc resin (0.05 mmol, 0.30 mmol g^{-1}) was used to synthesize this compound. After cleavage from the resin, the crude peptide was purified by preparative HPLC and was lyophilized to give a white solid (17.7 mg, 68%). ^{1}H NMR (500 MHz, DMSO-d_6, 25 °C): δ = 9.16 (d, 7.46 Hz, 1H), 8.11 (d, 7.08 Hz, 1H), 7.99 (s, 1H), 7.84 (d, 8.86 Hz, 1H), 7.80–7.77 (m, 2H), 7.67 (unresolved, 1H), 7.49–7.44 (m, 2H), 7.36 (s, 1H), 7.23 (s,1 H), 7.19 (s, 1H), 7.13 (s, 1H), 7.03 (s, 1H), 6.91 (s, 1H), 6.88 (s, 1H), 4.46–4.38 (m, 2H), 4.26–4.20 (m, 2H), 3.86–3.83 (m, 2H), 2.91–2.85 (m, 2H), 2.84–2.74 (m, 4H), 2.61 (dd, 8.01, 15.75 Hz, 1H), 2.22 (dd, 7.78, 12.77 Hz, 1H), 1.91–1.85 (m, 1H), 1.84–1.77 (m, 1H), 1.63–1.51 (m, 2H), 1.46–1.39 (m, 1H), 1.38–1.31 (m, 1H); analytical HPLC: homogeneous single peak, t_R = 8.19 min (8–70% B in 30 min); MALDI MS: calcd for $C_{25}H_{34}N_8O_7S$ $\{M+H\}^+$ 593.67, found $\{M+H\}^+$ 593.18.

4.12. ENN derivative 1k

TentaGel S RAM Fmoc resin (0.05 mmol, 0.30 mmol g^{-1}) was used to synthesize this compound. After cleavage from the resin, the crude peptide was purified by preparative HPLC and was lyophilized to give a white solid (13.7 mg, 46%). ^{1}H NMR (500 MHz, DMSO-d_6, 25 °C): δ = 12.07 (br s, 1H), 8.64 (d, 8.22 Hz, 1H), 8.21 (d, 7.91 Hz, 1H), 8.44 (d, 8.44 Hz, 1H), 8.02 (d, 7.60 Hz, 1H), 7.85 (s, 1H), 7.76–7.74 (m, 1H), 7.50–7.48 (m, 2H), 7.46–743 (m, 3H), 7.19 (s, 1H), 7.01 (s, 1H), 6.91 (s, 1H), 4.60–4.53 (m, 1H), 4.46–4.42 (m, 1H), 4.39–4.31 (m, 3H), 3.83–3.78 (m, 2H), 2.86 (dd, 6.93, 13.55 Hz, 1H), 2.69–2.66 (m, 1H), 2.59–2.56 (m, 2H), 2.40 (dd, 7.23, 13.55 Hz, 1H), 2.32 (t, 7.60, 2H), 2.09–2.02 (m, 1H), 1.94–1.85 (m, 1H); analytical HPLC: homogeneous single peak, t_R = 8.64 min (8–70% B in 30 min); MALDI MS: calcd for $C_{24}H_{31}N_7O_9S$ $\{M+Na\}^+$ 616.61, found $\{M+Na\}^+$ 616.11.

4.13. NKQ derivative 1l

TentaGel S RAM Fmoc resin (0.05 mmol, 0.30 mmol g^{-1}) was used to synthesize this compound. After cleavage from the resin, the crude peptide was purified by preparative HPLC and was lyophilized to give a white solid (10.8 mg, 36%). ^{1}H NMR (500 MHz, DMSO-d_6, 25 °C): δ = 8.55 (d, 7.94 Hz, 1H), 8.28 (d, 8.31 Hz, 1H), 8.19 (d, 7.22 Hz, 1H), 7.97 (d, 7.20 Hz, 1H), 7.81 (s, 1H), 7.71–7.68 (m, 3H), 7.53–7.50 (m, 3H), 7.46 (t, 7.65 Hz, 1H), 7.28 (s, 1H), 7.25 (s, 1H), 6.99 (s, 1H), 6.79 (s, 1H), 4.72–4.68 (m, 1H), 4.46–4.41 (m, 1H), 4.25–4.21 (m, 1H), 3.89–3.80 (m, 3H), 2.85 (dd, 6.83, 15.57 Hz, 1H), 2.79–2.74 (m, 2H), 2.67 (dd, 8.41, 13.25 Hz, 1H), 2.61 (dd, 6.53, 15.57 Hz, 1H), 2.29 (dd, 6.13, 13.25 Hz, 1H), 2.08 (t, 8.33 Hz, 2H), 1.96–1.87 (m, 2H), 1.86–1.77 (m, 2H), 1.59–1.46 (m, 2H), 1.40–1.25 (m, 2H); analytical HPLC: homogeneous single peak, t_R = 8.00 min (8–70% B in 30 min); MALDI MS: calcd for $C_{26}H_{38}N_8O_7S$ $\{M+H\}^+$ 607.70, found $\{M+H\}^+$ 607.23.

4.14. DNK derivative 1m

TentaGel S RAM Fmoc resin (0.05 mmol, 0.30 mmol g^{-1}) was used to synthesize this compound. After cleavage from the resin, the crude peptide was purified by preparative HPLC and was lyophilized to give a white solid (6.0 mg, 20%). ^{1}H NMR (500 MHz, DMSO-d_6, 25 °C): δ = 12.23 (br s, 1H), 8.16 (d, 7.11 Hz, 1H), 8.0 (s, 1H), 7.82 (d, 8.34 Hz, 1H), 7.79–7.77 (m, 1H), 7.75–7.68 (m, 3H), 7.5–7.45 (m, 2H), 7.36 (unresolved, 2H), 7.20 (s, 1H), 6.89 (s, 1H), 6.55 (s, 1H), 4.44–4.38 (m, 2H), 4.24–4.20 (m, 2H), 3.89–3.81 (m, 2H), 3.05–3.01 (m, 1H), 2.9–2.83 (m, 3H), 2.81–2.74 (m, 2H), 2.71–2.64 (m, 1H), 2.23–2.19 (m, 1H), 1.85–1.81 (m, 2H), 1.58–1.52 (m, 2H), 1.48–1.42 (m, 1H), 1.37–1.33 (m, 1H); analytical HPLC: homogeneous single peak, t_R = 9.17 min (8–70% B in 30 min); MALDI MS: calcd for $C_{25}H_{35}N_7O_8S$ $\{M+H\}^+$ 594.65, found $\{M+H\}^+$ 594.22.

4.15. CD experiments

CD measurements were obtained on an Aviv (model 62 DS) spectrometer. The peptidomimetics were dissolved in H_2O/MeOH (80:20) (c = 0.2 mg/mL, 0.1 cm path length). CD spectra were recorded at 25 °C.

4.16. NMR experiments

NMR spectra were recorded on either a Varian Inova 500 or Mercury 300 spectrometer (500 or 300 MHz, respectively, for ^{1}H; 125 or 75 MHz for ^{13}C). The concentrations of the samples were approximately 5 mg/mL in DMSO-d_6. One-dimensional (1D) ^{1}H NMR spectra were recorded with a spectral width of 8000 Hz, 32 transients, and a 3 s acquisition time. Vicinal coupling constants were measured from 1D spectra at 25 °C. Assignments of ^{1}H NMR resonances were performed using sequential connectivities. Temperature coefficients of the amide protons were measured via several 1D experiments in the temperature range of 25–55 °C adjusted in 5-degree increments with an equilibration time of about 10–15 min after successive rise in temperature.

Two-dimensional (2D) NMR spectra were recorded at 25 °C with a spectral width of 5000 Hz. Through-bond connectivities were elucidated by TOCSY and DQF-COSY spectra, which were recorded with 512 t_1 increments and 16 scans per t_1 increment, with 2K data points at t_2. Through-space interactions were identified by ROESY experiments, which were done under varying mixing times (100, 300, 400 ms). The one done with 300 ms mixing time proved superior over the others. The intensities of the ROESY cross peaks were assigned as strong (s), medium (m), and weak (w) from the magnitude of their volume integrals.

4.17. Molecular simulations

CHARMm (version 23.2, Molecular Simulations Inc.) was used for the molecular simulations performed in this work. Explicit atom representations were used throughout the study. The residue topology files (RTF) for all the peptidomimetics were built using QUANTA97 (Molecular Simulations Inc.).

Quenched molecular dynamics simulations were performed using the CHARMm standard parameters. Compounds **1a** and **1g** were modeled as cations (with positive charges localized on the lysine NH_3^+ side chain of **1a** and on the guanido group of arginine for **1g**) in a dielectric continuum of 45 (simulating DMSO). Thus, the starting conformers were minimized using 1000 steps of steepest descent (SD) and 3000 steps of the Adopted Basis Newton–Raphson method (ABNR), respectively. The minimized structures were then subjected to heating, equilibration, and dynamics simulation. Throughout, the equations of motions were integrated using the Verlet algorithm with a time step 1 fs, and SHAKE was used to constrain all bond lengths containing polar hydrogens. Each peptidomimetic was heated to 1000 K over 10 ps and equilibrated for another 10 ps at 1000 K, then molecular dynamics runs were performed for a total time of 600 ps with trajectories saved every 1 ps. The resulting 600 structures were thoroughly minimized using 1000 steps of SD followed by 3000 steps of ABNR until a RMS energy derivative of $\leqslant$0.01 kcal mol^{-1} $Å^{-1}$ was obtained. Structures with energies less than 3.0 kcal mol^{-1} relative to the global minimum were selected for further analysis.

The QUANTA97 package was again used to display, overlay, and classify the selected structures into conformational groups. The best clustering was obtained using a grouping method based on calculation of RMS deviation of a subset of atoms, in this study these were the ring backbone atoms. Thus, threshold cutoff values of 1.25 and 1.00 Å were selected for **1a** and **1g**, respectively, to obtain families with reasonable homogeneity. The lowest energy conformer from each family was considered as a typical representative of the family as a whole. Additionally, a second approach was also used to obtain a representation of each family. In this alternative

protocol, the coordinates of all the heavy atoms in each family were averaged in Cartesian space. The protons were re-built on those heavy atoms using standard geometries for each atom type, then the resulting structures were minimized using 50–100 steps of SD to smooth the bond lengths and angles. Finally, inter-proton distances and dihedral angles from both the lowest energy and the averaged structure were calculated for comparisons with the ROE data.

Acknowledgements

We thank Rapp Polymere, Argonaut Technologies, and Chiron Mimetopes for donating supports for this study. Financial support for this project was provided by the National Institutes of Health (CA82642), The Texas Advanced Technology Program, and the Robert A. Welch Foundation. TAMU/LBMS-Applications Laboratory headed by Dr Shane Stichy provided mass spectrometric support, and the Laboratory for Molecular Simulation's (Dr Lisa Thompson) supported our molecular simulations work. The NMR instrumentation in the Biomolecular NMR Laboratory at Texas A&M University was supported by a grant from the National Science Foundation (DBI-9970232) and the Texas A&M University System.

References

1. Jackson, S.; DeGrado, W.; Dwivedi, A.; Parthasarathy, A.; Higley, A.; Krywko, J.; Rockwell, A.; Markwalder, J.; Wells, G.; Wexler, R.; Mousa, S.; Harlow, R. *J. Am. Chem. Soc.* **1994**, *116*, 3220–3230.
2. Burgess, K. *Acc. Chem. Res.* **2001**, *34*, 826–835.
3. Lohof, E.; Planker, E.; Mang, C.; Burkhart, F.; Dechantsreiter, M. A.; Haubner, R.; Wester, H.-J.; Schwaiger, M.; Holzemann, G.; Goodman, S. L.; Kessler, H. *Angew. Chem., Int. Ed.* **2000**, *39*, 2761–2764.
4. Boer, J.; Gottschling, D.; Schuster, A.; Holzmann, B.; Kessler, H. *Angew. Chem., Int. Ed.* **2001**, *40*, 3870–3873.
5. Roedern, E. G. v.; Lohof, E.; Hessler, G.; Hoffmann, M.; Kessler, H. *J. Am. Chem. Soc.* **1996**, *118*, 10156–10167.
6. Roedern, E. G. v.; Kessler, H. *Angew. Chem., Int. Ed.* **1994**, *33*, 687–689.
7. Cochran, A. G. *Cur. Opin. Chem. Biol.* **2001**, *5*, 654–659.
8. Conte, L. L.; Chothia, C.; Janin, J. *J. Mol. Biol.* **1999**, *285*, 2177–2198.
9. Pattarawarapan, M.; Burgess, K. *J. Med. Chem.* **2003**, *46*, 5277–5291.
10. Feng, Y.; Pattarawarapan, M.; Wang, Z.; Burgess, K. *Org. Lett.* **1999**, *1*, 121–124.
11. Reyes, S.; Pattarawarapan, M.; Roy, S.; Burgess, K. *Tetrahedron* **2000**, *56*, 9809–9818.
12. Fields, G. B.; Noble, R. L. *Int. J. Peptide Protein Res.* **1990**, *35*, 161–214.
13. Patek, M. *Int. J. Peptide Protein Res.* **1993**, *42*, 97–117.
14. Guillier, F.; Orain, D.; Bradley, M. *Chem. Rev.* **2000**, *100*, 2091–2157.
15. NovaBiochem. *NovaBiochem Catalog & Peptide Synthesis Handbook*, 1999.
16. Litak, P. T.; Kaufmann, J. M. *J. Heterocycl. Chem.* **1994**, *31*, 457–479.
17. Stevens, E. S.; Sugawara, N.; Bonora, G. M.; Toniolo, C. *J. Am. Chem. Soc.* **1980**, *102*, 7048–7050.
18. Kessler, H.; Bats, J. W.; Griesinger, C.; Koll, S.; Will, M.; Wagner, K. *J. Am. Chem. Soc.* **1988**, *110*, 1033–1049.
19. O'Connor, S. D.; Smith, P. E.; Al-Obeidi, F.; Pettitt, B. M. *J. Med. Chem.* **1992**, *35*, 2870–2881.
20. Pettitt, B. M.; Matsunaga, T.; Al-Obeidi, F.; Gehrig, C.; Hruby, V. J.; Karplus, M. *Biophy. J. Biophys. Soc.* **1991**, *60*, 1540–1544.
21. Burgess, K.; Ho, K.-K.; Pettitt, B. M. *J. Am. Chem. Soc.* **1995**, *117*, 54–65.
22. Burgess, K.; Ho, K.-K.; Pal, B. *J. Am. Chem. Soc.* **1995**, *117*, 3808–3819.
23. Feng, Y.; Wang, Z.; Jin, S.; Burgess, K. *Chemistry—A European J.* **1999**, *5*, 3273–3278.
24. Wüthrich, K. *NMR of Proteins and Nucleic Acids*; Wiley: New York, 1986.
25. Bothner-By, A. A.; Stephen, R. L.; Lee, J.; Warren, C. D.; Jeanloz, R. W. *J. Am. Chem. Soc.* **1984**, *106*, 811–813.
26. Perczel, A.; Hollosi, M. In *Circular Dichroism and the Conformational Analysis of Biomolecules*; Fasman, G. D., Ed.; Plenum: New York and London, 1996; pp 362–364.
27. Kaiser, E.; Colescott, R. L.; Bossinger, C. D.; Cook, P. I. *Anal. BioChem.* **1970**, *34*, 595–598.